RESEARCH LETTER

Key Points:
- GrIS glacial meltwater residence times vary between 100 and 3600 years
- A lot of the GrIS glacial meltwater originates at altitudes between 1 and 2 km
- Most GrIS glacial meltwater is in disequilibrium with surface conditions

Supporting Information:
- Supporting Information S1

Correspondence to:
Yi Niu,
niuyi@umich.edu

Noble gas signatures in Greenland: Tracing glacial meltwater sources

Yi Niu[1], M. Clara Castro[1], Sarah M. Aciego[1], Chris M. Hall[1], Emily I. Stevenson[1], Carli A. Arendt[1], and Sarah B. Das[2]

[1]Department of Earth and Environmental Sciences, University of Michigan, Ann Arbor, Michigan, USA, [2]Woods Hole Oceanographic Institution, Woods Hole, Massachusetts, USA

Abstract This study represents the first comprehensive noble gas study in glacial meltwater from the Greenland Ice Sheet. It shows that most samples are in disequilibrium with surface collection conditions. A preliminary Ne and Xe analysis suggests that about half of the samples equilibrated at a temperature of ~0°C and altitudes between 1000 m and 2000 m, with a few samples pointing to lower equilibration altitudes and temperatures between 2°C and 5°C. Two samples suggest an origin as melted ice and complete lack of equilibration with surface conditions. A helium component analysis suggests that this glacial meltwater was isolated from the atmosphere prior to the 1950s, with most samples yielding residence times ≤420 years. Most samples represent a mixture between a dominant atmospheric component originating as precipitation and basal meltwater or groundwater, which has accumulated crustal ^{4}He over time.

1. Introduction

The study of noble gases (He, Ne, Ar, Kr, and Xe) dissolved in groundwater can enhance our understanding of surface and groundwater dynamics by providing us with an indication about flow paths, connectivity between aquifers, and water residence times [e.g., *Andrews*, 1985; *Mazor and Bosch*, 1992; *Castro et al.*, 1998a, 1998b; *Patriarche et al.*, 2004; *Castro et al.*, 2007]. In addition, because noble gases are conservative tracers and their concentrations in the recharge areas of groundwater systems are typically considered to be simply a function of temperature (*T*), pressure (*P*) (altitude of recharge area), and excess air (EA), noble gas temperatures (NGTs) have commonly been regarded as a potentially robust indicator of past climate [*Stute and Schlosser*, 1993; *Ballentine and Hall*, 1999; *Aeschbach-Hertig et al.*, 2002; *Kipfer et al.*, 2002; *Sun et al.*, 2010; *Castro et al.*, 2012].

Although noble gas studies have been carried out extensively in ice-free regions, studies of noble gases in glacial environments remain particularly scarce [e.g., *Craig and Wiens*, 1996; *Severinghaus and Battle*, 2006; *Malone et al.*, 2010]. High-latitude regions such as Greenland are extremely sensitive to and are significant drivers of climate change due to the enormous water masses they store. Understanding climate shifts in the Greenland Ice Sheet (GrIS) margins is even more critical as these areas may be particularly sensitive to global climate forcing [*Intergovernmental Panel on Climate Change*, 2013]. The GrIS has been extensively studied to estimate its ice melting and acceleration rates [*Rignot et al.*, 2011], as well as its contributions to sea level rise [*Zwally et al.*, 2005; *Shepherd and Wingham*, 2007; *Rignot et al.*, 2011]. However, many questions remain to be answered pertaining to the dynamics and seasonality of the GrIS [*Das et al.*, 2008; *Joughin et al.*, 2008], sources and composition of the meltwater, as well as temperature changes in GrIS and their driving mechanisms [*Hanna and Cappelen*, 2003; *Chylek et al.*, 2006].

Here, we present a pilot noble gas study of GrIS glacial meltwater. This study explores the information noble gases can provide in glacial environments with respect to glacial meltwater sources, relative source contributions, water residence times, and locations where this glacial meltwater originates within the ice sheet. Ultimately, we seek to improve our understanding of the dynamics of these massive ice sheets, critical for the major role they play in climate change. This is possible due to the conservative nature of noble gases and the temperature dependency of their concentrations in equilibrated air saturated water (ASW), allowing for calculation of NGTs and, under certain assumptions, estimation of the altitude at which glacial meltwater originated. In addition, crustally produced isotopes such as ^{4}He accumulate in water over time, allowing for a first-order estimation of water residence times.

2. Geology, Glaciology, and Climate

Greenland is located between the Arctic and Atlantic Oceans, northeast of Canada, and is covered by the GrIS. The Summit in central Greenland is 3231 m above sea level (asl); in southern Greenland, the highest elevation is 2873 m asl (Figure S1 in the supporting information) [*Bamber*, 2001]. The geology of the current ice-free margin has been extensively studied [e.g., *Baadsgaard*, 1973; *Friend and Nutman*, 2005; *Hollis et al.*, 2006; *Dawes*, 2009]. Most of the bedrock is Precambrian shield and is mainly composed of granitic gneiss and granitoids [*Dawes*, 2009].

Mean annual air temperatures range from −5°C to 2°C at our sampling locations (Figure S1). Average summer (June, July, and August) and winter (December, January, and February) temperatures observed within sea level to 100 m asl range from 5°C to 10°C and from −18°C to −4°C, respectively [*Vinther et al.*, 2006; *Hanna et al.*, 2012] (Danmarks Meteorologiske Institut, http://www.dmi.dk/groenland/arkiver/vejrarkiv/, 2014). Summer temperatures allow for surface melting to occur during a brief period.

3. Sampling and Analytic Methods

Thirteen samples for noble gas analysis were collected at five locations at or near the coast of central and southern Greenland (Figure S1) in July and August 2013, at or slightly after the peak of the summer melting season. These include eight subglacial (terminus) meltwater, three surface meltwater, and two river water samples. Samples were collected at altitudes between 0 and 1221 m asl with water collection temperatures ranging from 0°C to 2.8°C. Water samples were collected in standard refrigeration grade 3/8 in. copper tubing. All samples were analyzed at the Noble Gas Laboratory at the University of Michigan on a MAP-215 mass spectrometer following procedures described in *Castro et al.* [2009] and *Hall et al.* [2012].

4. Conceptual GrIS GMW Model: Implication for Noble Gases

Figure S2 illustrates a conceptual model of the GrIS glacial hydrology near the terminus area [*Martinerie et al.*, 1992, 1994; *Skidmore et al.*, 2005; *Das et al.*, 2008; *Cuffey and Paterson*, 2010]. Water starts as melted snow or firn at the surface, in contact with air. Partial noble gas equilibration may occur both at the surface (area a in Figure S2) and at the terminus area (area c in Figure S2). Exposure of surface GMW to the atmosphere varies between hours and weeks, where an ASW component forms. For example, the formation of a supraglacial lake over ~3–4 weeks was observed followed by massive and sudden drainage lasting ~1.4 h at an average rate of 8700 m^3/s [*Das et al.*, 2008]. EA is likely incorporated in GMW as water is fiercely transported through vertical conduits (crevasses and moulins), similar to the EA component present in sedimentary systems resulting from air bubbles trapped due to rapid water table fluctuations [*Heaton and Vogel*, 1981]. The meltwater discharged at the base of the glacier is likely a combination of surface melting routed through moulins and basal melt which has interacted with subglacial till and bedrock [*Jean-Baptiste et al.*, 2001; *Skidmore et al.*, 2005]. Trapped air in ice, which has a composition nearly indistinguishable from that of EA, can also be incorporated into the subglacial meltwater. This was observed by earlier studies of noble gases in ice cores and seawater affected by the submarine melting of ancient glacial ice [e.g., *Schlosser*, 1986; *Schlosser et al.*, 1990; *Martinerie et al.*, 1992, 1994; *Weppernig et al.*, 1996; *Hohmann et al.*, 2002; *Loose and Jenkins*, 2014]. Its contribution, however, following the local hydrologic conceptual model for the GrIS GMW (cf. Figure S2), is expected to be minor. The noble gas signature revealed by our samples supports this conceptual model (cf. section 5).

5. Results

Figure 1a displays noble gas concentrations of our samples normalized to those in 0.09 cm^3 of air per gram of ice, i.e., the expected trapped air in glacial ice [e.g., *Martinerie et al.*, 1992, 1994]. It is apparent that our samples are heavily depleted in Ne and present an extreme Xe enrichment when compared to trapped air in ice. These measured concentrations contrast highly with those of trapped air in ice and suggest that the bulk of our GrIS GMW is not derived directly from the melting of old glacial ice in absence of atmospheric contact. Figure 1b displays noble gas concentrations normalized to the ASW corresponding to measured water temperature and altitude at collection points. With the exception of He, for which buildup of radiogenic ^{4}He is observed, and in contrast to trapped air in ice, it is apparent that most samples display a pattern close
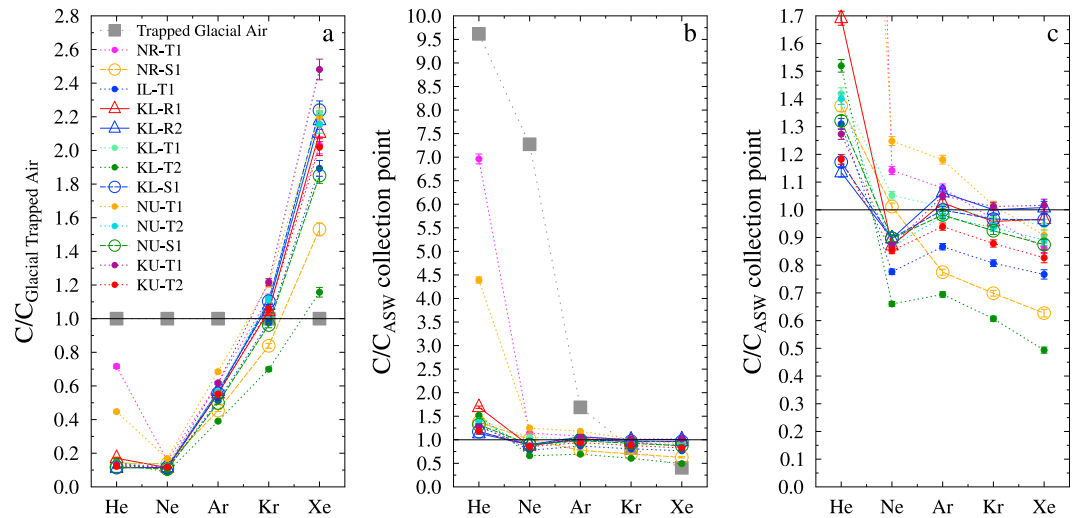
Figure 1. Measured noble gas concentrations normalized to (a) trapped air in glacier ice or (b and c) ASW at collection temperatures and altitudes. The solid black line indicates noble gas concentrations with no addition or loss of gases compared to trapped air in glacier ice or ASW. All samples (Figure 1b). Zoomed into 0–1.7 on the vertical axis (Figure 1c).

to that of ASW. This suggests that an ASW component largely dominates over any possible EA component, including one originating from trapped air in glacial ice for the four heavier noble gases. EA can be incorporated both during rapid transport through vertical conduits and from melted old glacial ice. The composition of these EA components are nearly identical.

From Figures 1b and 1c, it is apparent that for all GrIS GMW samples, noble gas concentrations do deviate somewhat from expected ASW values ($C/C_{ASW} = 1$) corresponding to measured water temperature and altitude at collection points (Figures 1b and 1c and Table S1). All samples display He excesses with respect to ASW values (Figure 1b). Two terminus samples (NR-T1 and NU-T1) display, by far, the highest excesses, with values up to 596% and 339% that of ASW, respectively (Figure 1b). All other samples display excesses varying between 14% and 69% that of ASW. The origin and respective fractions of these He excesses are constrained by R/R_a values, where R is the measured $^3He/^4He$ ratio and R_a is the atmospheric value of 1.384×10^{-6} [*Clarke et al.*, 1976]. All samples but KL-R2 display $R/R_a < 1$ (Table S1), pointing to the presence of a crustal He source ($0.02 \leq R_c/R_a \leq 0.05$) [e.g., *O'Nions and Oxburgh*, 1983] with a strong negative correlation between R/R_a values and total He concentrations (Figure S3). A decreasing trend of R_{exc}/R_a from atmospheric to crustal values with increased total He and $^4He_{exc}$ concentrations (where R_{exc} and $^4He_{exc}$ are the $^3He/^4He$ ratios and ^4He concentrations from which the atmospheric component was removed, respectively) [e.g., *Castro*, 2004] is also observed. This strongly suggests that ^4He excesses are dominated by ^4He crustal production, which allows, under certain assumptions, for subsequent calculation of GMW residence times (cf. section 6.2).In contrast to He, Ne, Kr, and Xe concentrations for most samples are depleted with respect to ASW, while six samples are also depleted in Ar (Figures 1b and 1c). Five samples are enriched in Ar up to a maximum of 18%, while two samples display expected ASW values with respect to collection point conditions. While Ne concentrations display a maximum depletion of 34%, Ar, Kr, and Xe display maximum depletions of 31%, 39%, and 51% with respect to ASW at collection altitudes and measured water temperatures. Deviations of measured concentrations from ASW values at collection point suggest an apparent lack of equilibration of GrIS meltwater with surface conditions (cf. section 6.1). The presence of two patterns in our samples is apparent. One group displays a mass-dependent depletion pattern with stronger depletion of the heavier noble gases compared to the lighter ones. This group consists of three terminus samples (NR-T1, KL-T1, and NU-T1) and one surface sample (NR-S1). Of these, three samples present Ne excesses, while sample NR-S1 displays the expected ASW Ne concentration. The second group displays a relative Ne depletion with respect to Ar, Kr, and Xe. This group includes nine samples of all three types, i.e., terminus, surface, and river samples. All samples in this group display Ne depletion with respect to ASW values at collection point conditions. As Ar, Kr, and Xe in GrIS GMW follow the mass-dependent depletion pattern for most samples, we refer here to this pattern as a relative Ne depletion as opposed to the relative Ar enrichment identified in previous
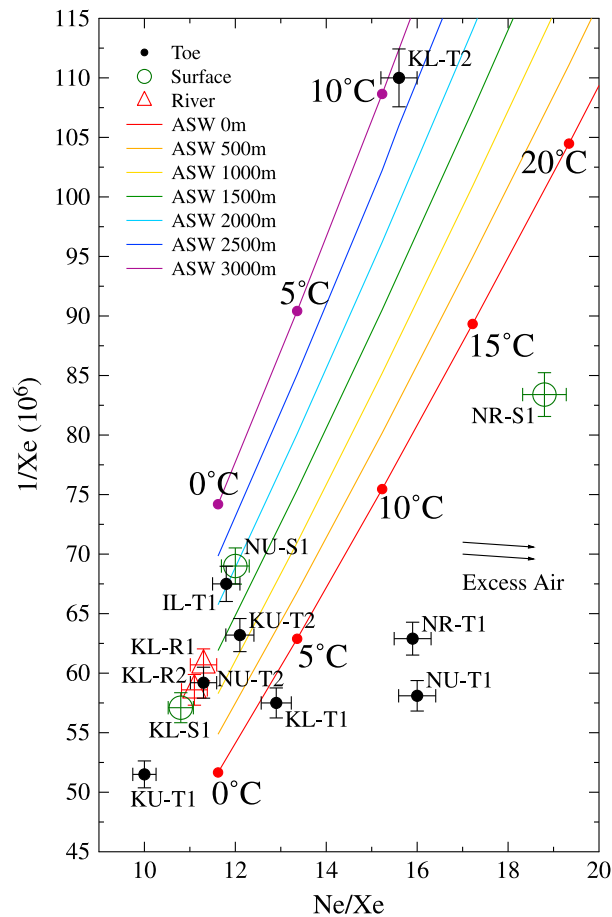
Figure 2. Preliminary estimation of equilibration temperatures and altitudes under the assumption that both Ne and Xe have equilibrated with surface conditions by comparing measured 1/Xe versus Ne/Xe for all Greenland samples with theoretical ASW values. Colored lines indicate ASW values at altitudes between 0 and 3000 m asl, and colored markers indicate temperatures between 0°C and 20°C. EA addition moves samples in the direction indicated by arrows.

studies [*Warrier et al.*, 2012, 2013]. All Ne, Ar, Kr, and Xe isotopic ratios are indistinguishable from ASW values. In their study of springs in the Galápagos Islands, *Warrier et al.* [2012] hypothesized that this mass-independent pattern is likely due to mixing between low-altitude (<~400 m) fog droplets and high-altitude precipitation. Fog was present in Greenland during two of our sampling days, and *Bergin et al.* [1994] have also reported the presence of fog at the Summit.

6. Discussion

6.1. Equilibration Temperatures and Altitudes

Concentrations of atmospheric noble gases dissolved in water record various physical parameters (e.g., temperature, EA, and altitude) at which final equilibration with the atmosphere takes place. Assuming that both Ne and Xe are in equilibrium with the atmosphere, it is possible to compare 1/Xe versus Ne/Xe to estimate an initial range of temperatures and altitudes of equilibration for our GrIS GMW samples [cf. *Warrier et al.*, 2012]. This is achieved by comparing measured Ne and Xe concentrations along with loci of calculated expected values for ASW for altitudes and temperatures varying between 0 and 3000 m asl and between 0°C and 20°C, respectively (Figure 2). Such a plot suggests that six samples (IL-T1, KL-R1, KL-R2, NU-T2, NU-S1, and KU-T2) have nearly equilibrated with the atmosphere at ~0°C
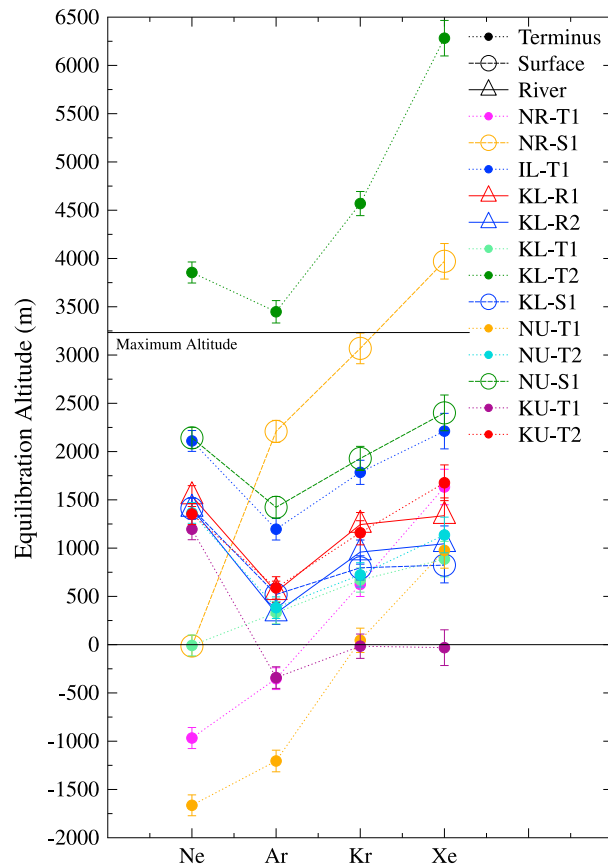
and at altitudes varying between 1000 m and 2000 m, values which are consistent with both temperatures and elevations in Greenland and, in particular, in our study area. In contrast, sample KL-T2, a terminus sample collected at 406 m at Kangerlussuaq (Figure S1), points to a significantly higher equilibration elevation, between 2500 m and 3000 m, and an apparent equilibration temperature of 11°C. This temperature is far too high and inconsistent with temperatures in the area and points to a lack of water equilibration with surface conditions. It is possible that the concentrations of the heavier noble gases and that of Xe in particular, which are extremely low in sample KL-T2, are due to ice formation at higher altitudes rather than the apparently high equilibration temperature. Indeed, due to their large atomic radii, Ar, Kr, and Xe tend to be excluded from the ice structure [*Top et al.*, 1988; *Malone et al.*, 2010]. Low heavy noble gas concentrations in precipitation have previously been observed and associated with ice formation at high altitudes [*Warrier et al.*, 2013]. Sample KL-T2 is likely to be melted ice that has not equilibrated with the atmosphere. In addition, samples KL-S1 and KU-T1 point to temperatures below freezing, which can be identified through their Ne depletion and/or Xe excess. On the other hand, samples NR-T1, NR-S1, KL-T1, and NU-T1 suggest the presence of EA as revealed by their excess Ne (Figure 2). Removing EA leads to lower apparent equilibration temperatures and higher apparent equilibration altitudes (cf. Text S1). More specifically, this leads to maximum equilibration temperatures of ~5°C, 2°C, and 3°C for samples NR-T1, KL-T1, and NU-T1, temperatures, which are consistent with conditions on the ground. Indeed, sample NR-T1 was collected at 25 m asl, very close to the observation site at Narsarsuaq [*Vinther et al.*, 2006; *Hanna et al.*, 2012], with a summer mean

Figure 3. Equilibration altitudes based on single gas concentrations assuming equilibration at 0℃. The black solid lines indicate the elevation interval physically possible based on Greenland topographic surface.

surface air temperature of ~10℃ [*Hanna et al.*, 2012]. Samples KL-T1 and NU-T1 were collected at 417 m asl and 176 m asl, respectively, at relative proximity to the observation site altitudes at Kangerlussuaq and Nuuk, respectively [*Vinther et al.*, 2006; *Hanna et al.*, 2012]. It is also possible for the equilibration temperature suggested by samples KL-T1 and NU-T1 to be compatible with the surface conditions. In contrast, sample NR-S1, collected at 176 m asl at Narsarsuaq, points to an equilibration temperature of ~13℃, assuming equilibrium at collection altitude. Similarly to sample KL-T2, this temperature is too high to be compatible with surface conditions in Greenland and suggests an ice origin, possibly melted ice which did not equilibrate with the atmosphere.

If equilibration for all noble gases is not warranted, as appears to be the case for at least some of our GrIS samples, examining each gas separately is necessary. Because Xe requires the longest equilibration times, it will provide us with the most reliable original equilibration altitudes. To determine equilibration altitudes based on each single noble gas, an equilibration temperature of 0℃ was assumed for all samples (Figure 3).

Overall, it is apparent from Figure 3 that 10 samples out of 13 yield Xe equilibration altitudes ranging from 820 m to 2400 m, an altitude interval that overlaps with that derived from Figure 2, but which is larger. Because the equilibration temperature is set at 0℃, higher apparent equilibration temperatures are equivalent to higher altitudes at lower temperatures. In particular, sample KL-T2 points to very high Ar, Kr, and Xe equilibration altitudes, which are higher than the highest elevation in Greenland. This reinforces the notion that sample KL-T2 is likely to have formed directly from ice and has not equilibrated with the atmosphere, as was previously discussed. Similarly, the Xe equilibration altitude of sample NR-S1, 4000 m, is also incompatible with conditions on the ground, pointing to melted ice that has not equilibrated with the atmosphere. However, Ar and Kr equilibration altitudes are compatible with Greenland topography and suggest that sample NR-S1 has reached a greater level of partial equilibration with the atmosphere than sample KL-T2. This sample's Ne equilibration altitude is approximately that of collection altitude and suggests that Ne equilibrated with the atmosphere at the time of collection. This, however, assumes the absence of EA. Three samples, KL-R1, KL-R2, and KL-S1, each shows very close Kr and Xe equilibration altitudes, which are also higher than their collection altitudes, suggesting that Kr has just started to equilibrate with surface conditions which are distinct from those at the water source, while Xe is still recording original water source altitudes. Xe equilibration altitude is higher than the collection altitude for sample KL-S1, suggesting that there is no Xe excess, and the apparent subfreezing temperature in Figure 2 is solely due to Ne depletion. On the other hand, Kr and Xe of sample KU-T1 have equilibrated with surface conditions at the collection point, preventing identification of this water's original source. Similar to sample KL-S1, its anomalously low Ne concentration, shown as high equilibration altitude in Figure 3, causes the apparent subfreezing temperature in Figure 2. Three samples, NR-T1, KL-T1, and NU-T1, yield Ne equilibration altitudes at or below sea level and thus below their collection altitudes, suggesting the presence of Ne excess resulting from EA.
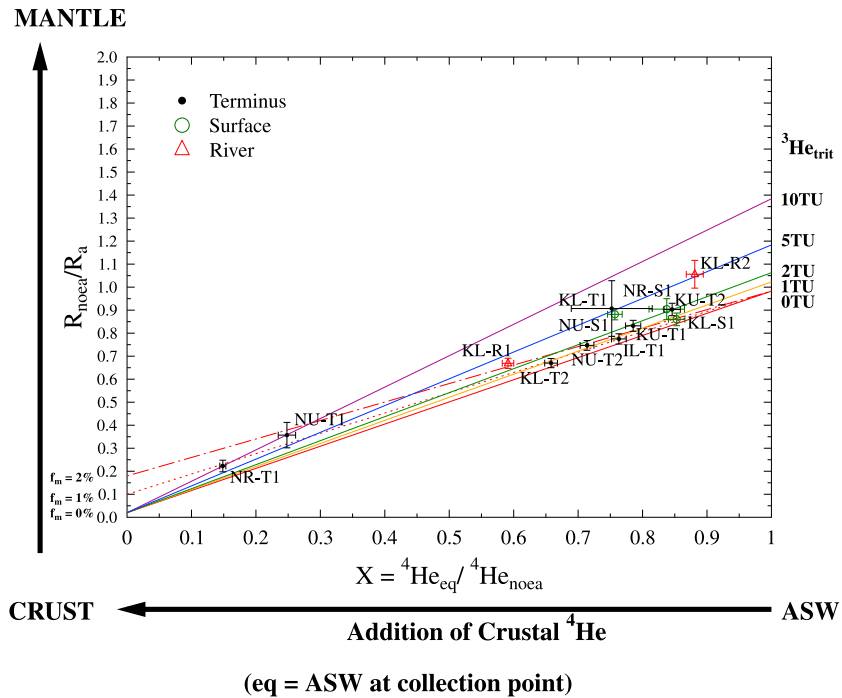
Figure 4. Helium component separation. Colored lines indicate expected position for samples with tritiogenic [3]He levels varying from 0 to 10 TU and percentages of mantle component in the non-ASW sources varying between 0% and 2%. The terms f_m noted along the left vertical axis indicate mantle contributions to the He in the sums of crustal and mantle sources. End-members used for crust and mantle components are 0.02 and 8 times the atmospheric value, respectively. The x coordinate indicates the fraction of He contributed by ASW. The total contributions of crustal and mantle source are calculated by subtracting the x coordinates from 1, denoted as $(1 - X)$. Mantle contribution to the whole sample is the corresponding f_m multiplied by $(1 - X)$.

As Ne concentration is greatly affected by the EA component, a negative EA component or a degassing process may be required to explain the observed Ne depletion. Bubbles that form in water under pressure and subsequently escape from the water phase are likely to preferentially lower Ne concentrations dissolved in water. *Warrier et al.* [2012] hypothesized that higher pressures in fog droplets cause lower noble gases solubilities in fog than the surrounding air. Due to Ne's higher diffusivity, Ne is more sensitive to pressure differences than the heavier noble gases, resulting in lower Ne concentrations relative to heavier noble gases. Subsequent mixing of the fog with ASW components might lead to Ne depletion. This process could partially explain the relative Ne depletion and Ar enrichment observed in some of our samples.

6.2. Sources and Residence Times of GrIS Meltwater

It is possible to separate and quantify the different He components, i.e., atmospheric, crustal, and/or mantle to identify different water sources, i.e., precipitation as rain, snow, or ice versus groundwater. Estimation of the crustal He component subsequently allows estimation of groundwater residence times under certain simplifications and assumptions. This analysis is typically done by plotting R_{noea}/R_a versus $^4He_{eq}/^4He_{noea}$, where R_{noea} and $^4He_{noea}$ are the $^3He/^4He$ ratios and total measured ^4He concentration at collection conditions after removal of EA and $^4He_{equation}$ is the ASW ^4He concentration under collection conditions (Figure 4) [*Castro*, 2004] (Text S2). From Figure 4, it is apparent that two terminus samples, NR-T1 and NU-T1, are dominated by crustal ^4He. These samples have crustal contributions of 84.4% and 74.0%, minor mantle contributions of 0.7%–1.2%, and likely premodern atmospheric contributions of 14.9% and 24.8%, respectively, as indicated by a complete absence of tritiogenic ^3He. Alternatively, 10 tritium unit (TU) could be considered in the absence of a mantle component. However, due to the significant amounts of crustal ^4He in these samples, this scenario is unlikely as 10 TU would correspond to modern water, which cannot have built up ^4He. Indeed, measurements of tritium levels in Greenland precipitation in 2009 show an annual average value of 11 TU (International Atomic Energy Agency, https://www.univie.ac.at/cartography/project/wiser/, 2012).

All other samples are dominated by an ASW component with $^3He_{trit}$ levels varying between 0 TU and 5 TU, lower than modern average tritium values (Figure 4). The very low $^3He_{trit}$ levels suggest that (1) our glacial meltwater samples have been isolated from contact with the atmosphere since before the bomb-test era, i.e., prior to the 1950s or (2) samples are very young so tritium has not yet decayed. Our first-order glacial meltwater residence time estimation based on $^4He_{exc}$ concentrations, together with estimated ^4He production rates in basement rocks and ^4He accumulation rates in water (Text S3), supports scenario 1, as very young water would not have accumulated radiogenic ^4He from contact with bedrock. Based on excess ^4He concentrations and ^4He production rates, maximum and minimum water residence times were calculated (Text S3 and Table S2). Average ^4He water ages were also estimated (Text S3 and Table S2). It should be noted that these age estimations yield simply a first estimation for the GMW. Although most samples display residence times between 100 years and 420 years, terminus samples NR-T1 and NU-T1 display significantly older ages of 3600 years and 1900 years, respectively. These residence times further support the notion that the ice from which these samples originated was isolated from the atmosphere prior to the 1950s. Highly variable calculated ages reflect the dominance of various contributions and origins for different samples, in particular, the presence of an older crustal versus a younger atmospheric component.

Overall, the atmospheric component dominates, with most samples displaying an atmospheric ASW contribution of ~59%–88% and a crustal contribution of ~12%–41%. This suggests that at least 59%–88% of the water is from precipitation as liquid, snow, or ice, with the remainder being meltwater either from the base of the ice sheet that has accumulated ^4He over time or directly from groundwater moving upward, a process commonly observed in crystalline, fractured systems. Processes such as upward He diffusion are not considered, rendering these fractions representative of lower limits, and they may be underestimated. The two terminus samples with ~84% and ~74% crustal ^4He suggest that much of this water is from basal melt or groundwater that has accumulated crustal ^4He for a much longer time period, with possibly additional mantle He. Mixing of groundwater with basal meltwater will lead to overestimated basal meltwater residence times and older apparent ages.

References

Aeschbach-Hertig, W., M. Stute, J. F. Clark, R. F. Reuter, and P. Schlosser (2002), A paleotemperature record derived from dissolved noble gases in groundwater of the Aquia Aquifer (Maryland, USA), *Geochim. Cosmochim. Acta*, *66*(5), 797–817.

Andrews, J. N. (1985), The isotopic composition of radiogenic helium and its use to study groundwater movement in confined aquifers, *Chem. Geol.*, *49*(1), 339–351.

Baadsgaard, H. (1973), U-Th-Pb dates on zircons from the early Precambrian Amîtsoq gneisses, Godthaab district, West Greenland, *Earth Planet. Sci. Lett.*, *19*(1), 22–28.

Ballentine, C. J., and C. M. Hall (1999), Determining paleotemperature and other variables by using an error-weighted, nonlinear inversion of noble gas concentrations in water, *Geochim. Cosmochim. Acta*, *63*(16), 2315–2336.

Bamber, J. (2001), *Greenland 5 km DEM, Ice Thickness, and Bedrock Elevation Grids*, NASA Nat. Snow and Ice Data Center Distrib. Active Archive Center, Boulder, Colo.

Bergin, M. H., J. L. Jaffrezo, C. I. Davidson, R. Caldow, and J. Dibb (1994), Fluxes of chemical species to the Greenland ice sheet at Summit by fog and dry deposition, *Geochim. Cosmochim. Acta*, *58*(15), 3207–3215.

Castro, M. C. (2004), Helium sources in passive margin aquifers—New evidence for a significant mantle ^3He source in aquifers with unexpectedly low in situ $^3He/^4He$ production, *Earth Planet. Sci. Lett.*, *222*(3), 897–913.

Castro, M. C., A. Jambon, G. Marsily, and P. Schlosser (1998a), Noble gases as natural tracers of water circulation in the Paris Basin: 1. Measurements and discussion of their origin and mechanisms of vertical transport in the basin, *Water Resour. Res.*, *34*(10), 2443–2466, doi:10.1029/98WR01956.

Castro, M. C., P. Goblet, E. Ledoux, S. Violette, and G. Marsily (1998b), Noble gases as natural tracers of water circulation in the Paris Basin: 2. Calibration of a groundwater flow model using noble gas isotope data, *Water Resour. Res.*, *34*(10), 2467–2483, doi:10.1029/98WR01957.

Castro, M. C., C. M. Hall, D. Patriarche, P. Goblet, and B. R. Ellis (2007), A new noble gas paleoclimate record in Texas—Basic assumptions revisited, *Earth Planet. Sci. Lett.*, *257*(1), 170–187.

Castro, M. C., L. Ma, and C. M. Hall (2009), A primordial, solar He–Ne signature in crustal fluids of a stable continental region, *Earth Planet. Sci. Lett.*, *279*(3), 174–184.

Castro, M. C., R. B. Warrier, C. M. Hall, and K. Lohmann (2012), A late Pleistocene–Mid-Holocene noble gas and stable isotope climate and subglacial record in southern Michigan, *Geophys. Res. Lett.*, *39*, L19709, doi:10.1029/2012GL053098.

Chylek, P., M. K. Dubey, and G. Lesins (2006), Greenland warming of 1920–1930 and 1995–2005, *Water Resour. Res.*, *33*, L11707, doi:10.1029/2006GL026510.

Clarke, W. B., W. J. Jenkins, and Z. Top (1976), Determination of tritium by mass spectrometric measurement of ^3He, *Int. J. Appl. Radiat. Isot.*, *27*(9), 515–522.

Craig, H., and R. C. Wiens (1996), Gravitational enrichment of $^{84}Kr/^{36}Ar$ ratios in polar ice caps: A measure of firn thickness and accumulation temperature, *Science*, *271*(5256), 1708–1710.

Cuffey, K. M., and W. S. B. Paterson (2010), *The Physics of Glaciers*, Academic, Amsterdam.

Das, S. B., I. Joughin, M. D. Behn, I. M. Howat, M. A. King, D. Lizarralde, and M. P. Bhatia (2008), Fracture propagation to the base of the Greenland ice sheet during supraglacial lake drainage, *Science*, *320*(5877), 778–781.

Dawes, P. R. (2009), The bedrock geology under the Inland Ice: The next major challenge for Greenland mapping, *Geol. Surv. Denmark and Greenland Bull.*, *17*, 57–60.

Friend, C. R., and A. P. Nutman (2005), New pieces to the Archaean terrane jigsaw puzzle in the Nuuk region, southern West Greenland: Steps in transforming a simple insight into a complex regional tectonothermal model, *J. Geol. Soc.*, *162*(1), 147–162.

Hall, C. M., M. Castro, K. C. Lohmann, and T. Sun (2012), Testing the noble gas paleothermometer with a yearlong study of groundwater noble gases in an instrumented monitoring well, *Water Resour. Res.*, *48*, W04517, doi:10.1029/2011WR010951.

Hanna, E., and J. Cappelen (2003), Recent cooling in coastal southern Greenland and relation with the North Atlantic Oscillation, *Geophys. Res. Lett.*, *30*(3), 1132, doi:10.1029/2002GL015797.

Hanna, E., S. H. Mernild, J. Cappelen, and K. Steffen (2012), Recent warming in Greenland in a long-term instrumental (1881–2012) climatic context: I. Evaluation of surface air temperature records, *Environ. Res. Lett.*, *7*(4), 045404.

Heaton, T. H. E., and J. C. Vogel (1981), "Excess air" in groundwater, *J. Hydrol.*, *50*, 201–216.

Hohmann, R., P. Schlosser, S. Jacobs, A. Ludin, and R. Weppernig (2002), Excess helium and neon in the southeast Pacific: Tracers for glacial meltwater, *J. Geophys. Res.*, *107*(C11), 3198, doi:10.1029/2000JC000378.

Hollis, J. A., D. Frei, J. A. van Gool, A. A. Garde, and M. Persson (2006), Using zircon geochronology to resolve the Archaean geology of southern West Greenland, *Geol. Surv. Denmark and Greenland Bull.*, *10*, 49–52.

Intergovernmental Panel on Climate Change (2013), *Climate Change 2013: The Physical Science Basis. Contribution of Working Group I to the Fifth Assessment Report of the Intergovernmental Panel on Climate Change*, edited by T. F. Stocker et al., 1535 pp., Cambridge Univ. Press, Cambridge, U. K., and New York, doi:10.1017/CBO9781107415324.

Jean-Baptiste, P., J. R. Petit, V. Y. Lipenkov, D. Raynaud, and N. I. Barkov (2001), Constraints on hydrothermal processes and water exchange in Lake Vostok from helium isotopes, *Nature*, *411*(6836), 460–462.

Joughin, I., S. B. Das, M. A. King, B. E. Smith, I. M. Howat, and T. Moon (2008), Seasonal speedup along the western flank of the Greenland Ice Sheet, *Science*, *320*(5877), 781–783.

Kipfer, R., W. Aeschbach-Hertig, F. Peeters, and M. Stute (2002), Noble gases in lakes and ground waters, *Rev. Mineral. Geochem.*, *47*(1), 615–700.

Loose, B., and W. J. Jenkins (2014), The five stable noble gases are sensitive unambiguous tracers of glacial meltwater, *Geophys. Res. Lett.*, *41*, 2835–2841, doi:10.1002/2013GL058804.

Malone, J. L., M. C. Castro, C. M. Hall, P. T. Doran, F. Kenig, and C. P. McKay (2010), New insights into the origin and evolution of Lake Vida, McMurdo Dry Valleys, Antarctica—A noble gas study in ice and brines, *Earth Planet. Sci. Lett.*, *289*(1), 112–122.

Martinerie, P., D. Raynaud, D. M. Etheridge, J. M. Barnola, and D. Mazaudier (1992), Physical and climatic parameters which influence the air content in polar ice, *Earth Planet. Sci. Lett.*, *112*(1), 1–13.

Martinerie, P., V. Y. Lipenkov, D. Raynaud, J. Chappellaz, N. I. Barkov, and C. Lorius (1994), Air content paleo record in the Vostok ice core (Antarctica): A mixed record of climatic and glaciological parameters, *J. Geophys. Res.*, *99*(D5), 10,565–10,576, doi:10.1029/93JD03223.

Mazor, E., and A. Bosch (1992), Helium as a semi-quantitative tool for groundwater dating in the range of 10^4–10^8 years, in *Isotopes of Noble Gases as Tracers in Environmental Studies*, pp. 163–178, IAEA, Vienna.

O'Nions, R. K., and E. R. Oxburgh (1983), Heat and helium in the Earth, *Nature*, *306*(5942), 429–431.

Patriarche, D., M. C. Castro, and P. Goblet (2004), Large-scale hydraulic conductivities inferred from three-dimensional groundwater flow and ^{4}He transport modeling in the Carrizo aquifer, Texas, *J. Geophys. Res.*, *109*, B11202, doi:10.1029/2004JB003173.

Rignot, E., I. Velicogna, M. R. Van den Broeke, A. Monaghan, and J. T. M. Lenaerts (2011), Acceleration of the contribution of the Greenland and Antarctic ice sheets to sea level rise, *Geophys. Res. Lett.*, *38*, L05503, doi:10.1029/2011GL046583.

Schlosser, P. (1986), Helium: A new tracer in Antarctic oceanography, *Nature*, *321*, 233–235.

Schlosser, P., R. Bayer, A. Foldvik, T. Gammelsrød, G. Rohardt, and K. O. Münnich (1990), Oxygen 18 and helium as tracers of ice shelf water and water/ice interaction in the Weddell Sea, *J. Geophys. Res.*, *95*(C3), 3253–3263, doi:10.1029/JC095iC03p03253.

Severinghaus, J. P., and M. O. Battle (2006), Fractionation of gases in polar ice during bubble close-off: New constraints from firn air Ne, Kr and Xe observations, *Earth Planet. Sci. Lett.*, *244*(1), 474–500.

Shepherd, A., and D. Wingham (2007), Recent sea-level contributions of the Antarctic and Greenland ice sheets, *Science*, *315*(5818), 1529–1532.

Skidmore, M., S. P. Anderson, M. Sharp, J. Foght, and B. D. Lanoil (2005), Comparison of microbial community compositions of two subglacial environments reveals a possible role for microbes in chemical weathering processes, *Appl. Environ. Microbiol.*, *71*(11), 6986–6997.

Stute, M., and P. Schlosser (1993), Principles and applications of the noble gas paleothermometer, *Clim. Change Cont. Isot. Rec.*, *78*, 89–100.

Sun, T., C. M. Hall, and M. C. Castro (2010), Statistical properties of groundwater noble gas paleoclimate models: Are they robust and unbiased estimators?, *Geochem. Geophys. Geosyst.*, *11*, Q02002, doi:10.1029/2009GC002737.

Top, Z., S. Martin, and P. Becker (1988), A laboratory study of dissolved noble gas anomaly due to ice formation, *Geophys. Res. Lett.*, *15*(8), 796–799, doi:10.1029/GL015i008p00796.

Vinther, B. M., K. K. Andersen, P. D. Jones, K. R. Briffa, and J. Cappelen (2006), Extending Greenland temperature records into the late eighteenth century, *J. Geophys. Res.*, *111*, D11105, doi:10.1029/2005JD006810.

Warrier, R. B., M. C. Castro, and C. M. Hall (2012), Recharge and source-water insights from the Galapagos Islands using noble gases and stable isotopes, *Water Resour. Res.*, *48*, W03508, doi:10.1029/2011WR010954.

Warrier, R. B., M. Clara Castro, C. M. Hall, and K. C. Lohmann (2013), Noble gas composition in rainwater and associated weather patterns, *Geophys. Res. Lett.*, *40*, 3248–3252, doi:10.1002/grl.50610.

Weppernig, R., P. Schlosser, S. Khatiwala, and R. G. Fairbanks (1996), Isotope data from Ice Station Weddell: Implications for deep water formation in the Weddell Sea, *J. Geophys. Res.*, *101*, 25–723, doi:10.1029/96JC01895.

Zwally, H. J., M. B. Giovinetto, J. Li, H. G. Cornejo, M. A. Beckley, A. C. Brenner, J. L. Saba, and D. Yi (2005), Mass changes of the Greenland and Antarctic ice sheets and shelves and contributions to sea-level rise: 1992–2002, *J. Glaciol.*, *51*(175), 509–527.